ACS APPLIED MATERIALS & INTERFACES

RESEARCH ARTICLE

www.acsami.org

Zwitterionic Sulfobetaine-Grafted Poly(vinylidene fluoride) Membrane with Highly Effective Blood Compatibility via Atmospheric Plasma-Induced Surface Copolymerization

Yung Chang,* Wan-Ju Chang, Yu-Ju Shih, Ta-Chin Wei, and Ging-Ho Hsiue

R&D Center for Membrane Technology and Department of Chemical Engineering, Chung Yuan Christian University, Chung-Li, Taoyuan 320, Taiwan

ABSTRACT: Development of nonfouling membranes to prevent nonspecific protein adsorption and platelet adhesion is critical for many biomedical applications. It is always a challenge to control the surface graft copolymerization of a highly polar monomer from the highly hydrophobic surface of a fluoropolymer membrane. In this work, the blood compatibility of poly(vinylidene fluoride) (PVDF) membranes with surface-grafted electrically neutral zwitterionic poly(sulfobetaine methacrylate) (PSBMA), from atmospheric plasma-induced surface copolymerization, was studied. The effect of surface composition and graft morphology, electrical neutrality, hydrophilicity and hydration capability on blood compatibility of the membranes were determined. Blood compatibility of the zwitterionic PVDF membranes was systematically evaluated by plasma protein adsorption, platelet adhesion, plasma-clotting time, and blood cell hemolysis. It was found that the nonfouling nature and hydration capability of grafted PSBMA polymers can be effectively controlled by regulating the grafting coverage and charge balance of the PSBMA layer on the PVDF membrane surface. Even a slight charge bias in the grafted zwitterionic PSBMA layer can induce electrostatic interactions between proteins and the membrane surfaces, leading to surface protein adsorption, platelet activation, plasma clotting and blood cell hemolysis. Thus, the optimized PSBMA surface graft layer in overall charge neutrality has a high hydration capability and the best antifouling, anticoagulant, and antihemolytic activities when comes into contact with human blood.

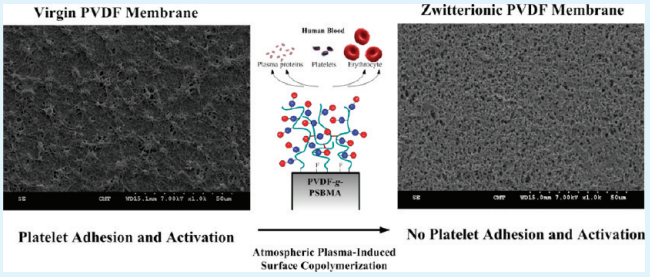

KEYWORDS: zwitterionic, nonfouling, atmospheric plasma, poly(vinylidene fluoride), sulfobetaine, blood compatibility

INTRODUCTION

Nonfouling materials have an important medical application as blood-compatible devices, which are highly desirable in the design of hemodialysis membranes, antithrombogenic implants, and biosensors used in contact with human blood.[1−10] The incorporation of a potent platelet inhibitor, heparin, onto the material surface is the most popular technique for minimizing the thrombogenicity of materials. In this regard, it is well-known that the heparinized surfaces have anticoagulant properties that prolong blood clotting time when they are coated on blood devices or containers.[3] However, only a few synthetic candidates are regarded as good blood-compatible materials.[11] In general, it is acknowledged that nonspecific protein adsorption is the first interaction event that occurs at the interface between materials and human blood. Some specific proteins in blood, such as fibrinogen and clotting enzymes, play an important role in material-induced clotting.[12,13] For example, even a small amount of fibrinogen adsorbed on a material surface may induce a multistep and interlinked process, including platelet adhesion and activation, and clot formation. Thus, good nonspecific protein resistance is one of the key requirements for synthetic nonfouling materials. Zwitterionic polymers containing the pendant groups of phosphobetaine, sulfobetaine, and carboxybetaine have received growing attention for use in the new generation of blood inert materials because of their good plasma protein resistance.[4,5,7−9,14−23] A general characteristic of the zwitterionic structure is the fact that they have both a positively and a negatively charged moiety within the same segment side chain, but maintain overall charge neutrality. The structure of sulfobetaine is similar to that of taurine betaine, which plays an important role in numerous physiological functions. In recent years, zwitterionic poly(sulfobetaine methacrylate) (PSBMA) has become the most widely studied zwitterionic polymer due to its ease in synthetic preparation.[5] Our previous work reported that zwitterionic PSBMA is an effective and stable nonfouling material that provides a surface for protein-fouling resistance and has excellent blood compatibility with human whole blood at physiologic temperature.[18−23] It was also reported that the nonfouling nature of PSBMA polymers is attributed to their highly hydration capabilities and conformational structures.[21,22]

In general, surface modification is considered as a promising approach to incorporate nonfouling materials onto a wide range of hydrophobic substrates for improved hemocompatibility.[4,8−10] Therefore, a new generation of blood-compatible membranes can be designed with a combination of the excellent mechanical

Received: January 16, 2011
Accepted: March 10, 2011
Published: March 10, 2011

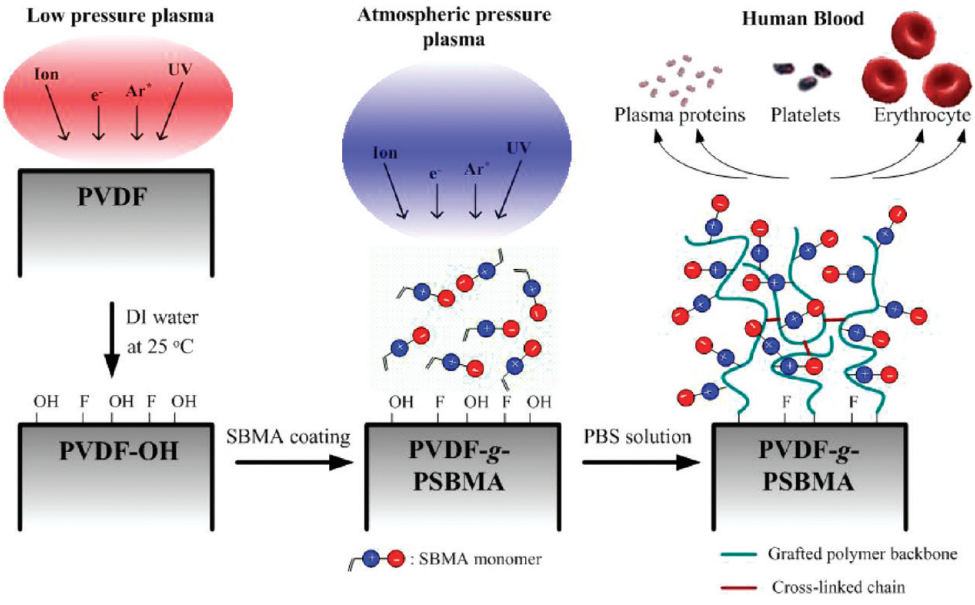

Figure 1. Schematic illustration of the preparation process of the zwitterionic PVDF-*g*-PSBMA membranes via atmospheric plasma-induced surface copolymerization.

bulk properties of hydrophobic materials and the good nonfouling surface characteristics of zwitterionic polymer layers, such as PSBMA.[17,19,24−28] Fluoropolymer membranes exhibit a wide range of outstanding properties, including strong mechanical strength, high-temperature stability, excellent chemical resistance, and low water sorption.[29,30] Various surface modification techniques have been proposed to design fluoropolymer materials with specific functional groups, such as chemical, plasma, irradiation, corona discharge, and flame treatments.[31,32] It is challenging to control the surface grafting of highly polar zwitterionic polymer, PSBMA, into the chemically inert and hydrophobic surface of a fluoropolymer membrane, poly(vinylene fluoro) (PVDF). Recently, a few studies have reported a successful modification process for the PVDF membrane surface-grafted with the zwitterionic PSBMA polymer layer (PVDF-g-PSBMA).[31] Prof. Kang first demonstrated surface modification of PVDF-g-PSBMA using thermally induced molecular graft copolymerization of the zwitterionic monomer with the ozone-preactivated PVDF that was carried out in a mixed solvent. Our previous work also demonstrated the surface modification of PVDF-g-PSBMA using ozone surface activation and surface-initiated atom transfer radical polymerization (ATRP).[32] However, previous approaches lack efficient grafting control (e.g., low grafting yield and long modification time) to process the surface copolymerization of zwitterionic monomers on PVDF membranes. Herein, a new interfacial process of atmospheric plasma-induced surface copolymerization was developed to control the surface modification of PVDF membranes grafted with zwitterionic PSBMA polymer and was used for the general application of devices that come into contact with blood.

Previous studies showed that the control of surface grafting coverage of zwitterionic layers is important for modified substrate with a blood-compatible interface.[6,17] Our study showed that it is significant to keep the charge neutrality of grafted polymer in minimizing the electrostatic interactions with plasma proteins and blood cells.[21] In addition, the formation of the bounded water layer on a highly hydrated surface was also demonstrated as a crucial issue to repel plasma proteins and made the antithrombogenic surface generated.[22,33,34] In general, plasma treatment usually results in the chemical degradation of grafted polymer because of the high energy of ion bombardment or UV radiation.[32,35] However, at present there still unclear about the control of zwitterionic grafted layer on highly hydrophobic surface with charge neutrality and high hydrophilicity via plasma-induced surface copolymerization. In this work, we extend our previous studies to propose a new insight of controlled charge neutrality on the PVDF membrane grafted with zwitterionic PSBMA polymer layer via a new process of atmospheric plasma-induced surface copolymerization. The effect of different plasma treating time and grafting yields of PSBMA polymer on the surface composition, grafting morphology, electrical neutrality, hydrophilicity and hydration capability of PVDF-*g*-PSBMA membranes were discussed in detail. This study also systematically demonstrated the blood compatibility of PVDF-*g*-PSBMA membranes evaluated by the plasma protein adsorption, platelet adhesion, plasma-clotting time, and blood cell hemolysis. The most important issue of this work is aimed to clarify the scientific correlations between interfacial grafting structures of zwitterionic PSBMA polymer layer and blood compatibility of PSBMA-grafted PVDF membranes via atmospheric plasma-induced surface copolymerization. Importantly, results indicate that PVDF-*g*-PSBMA membrane exhibited a hemocompatible character for plasma-protein and blood-platelet resistance that strongly depended on the surface hydrophilicity and charge-bias of the zwitterionic PSBMA layer on PVDF membranes.

EXPERIMENTAL SECTION

Materials. PVDF microporous membranes with an average pore size of 0.1 μm, a thickness of approximately 110 μm, and a diameter of 47 mm were purchased from the Millipore Co. (VVHP04700) and were used as received. [2-(Methacryloyloxy)ethyl] dimethyl(3-sulfopropyl)-ammonium hydroxide (sulfobetaine methacrylate, SBMA) macromonomer was purchased from Monomer-Polymer & Dajac Laboratories,

Inc.. Isopropanol (IPA) was obtained from Sigma-Aldrich and was used as a solvent for the plasma-induced graft-polymerization. Fibrinogen (fraction I from human plasma) was purchased from Sigma Chemical Co. Human blood and plasma solution were obtained from the Taiwan Blood Services Foundation. Phosphate buffer saline (PBS) was purchased from Sigma-Aldrich. Deionized water used in the experiments was purified using a Millipore water purification system with a minimum resistivity of 18.0 MΩ m.

Surface Copolymerization. A schematic illustration of the plasma-induced surface copolymerization of zwitterionic PSBMA on PVDF membranes under the control of integrated plasma treatment is shown in Figure 1. The PVDF membrane was first treated by low-pressure plasma with an argon flow rate of 10 slm and input power of 100 W controlled by a 13.56 MHz RF generator (Cesar 136, Dressler). The post-treated PVDF membrane with a surface area of approximately 0.4 cm^2 was incubated in a methanol solution containing 30 wt % SBMA monomer. After the SBMA-coated PVDF membrane was dried at 25 °C for 24 h, the membrane coated with the SBMA monomer layer of ~2.0 mg/cm^2 was then followed by atmospheric plasma treatment with an argon flow rate of 10 slm and input power of 150 W controlled by a 13.56 MHz RF generator. After plasma treatment, the zwitterionic PVDF membrane was transferred into purified methanol and was then extracted with deionized water and methanol, respectively, each for 60 min in the ultrasonic device to strip off PSBMA homopolymers and unreacted monomers. The residual solvent was removed in a vacuum oven under reduced pressure for 1 day and dried in a freeze-dryer at −45 °C for 1 day. In this study, all membranes after plasma treatment were cleaned using the same postwash procedures. The surface grafting yield (mg/cm^2) of the modified PVDF membrane is defined as the weight difference between the modified PVDF membrane and the virgin PVDF membrane divided by the surface area of the virgin PVDF membrane.

Surface Characterization. The chemical composition of surface-modified PVDF membranes with grafted PSBMA layer was characterized using FT-IR spectrophotometer (Perkin-Elmer Spectrum One) with ZnSe as an internal reflection element. Each spectrum was captured by averaging 32 scans at a resolution of 4 cm^{-1}. The surface grafting yield of PSBMA on the PVDF membrane was determined by the extent of weight increase compared to the virgin PVDF membrane based on the unit surface area 1 cm^2 of PVDF membrane. Prior to the weight measurements, the membranes were dried in a freeze-dryer at −45 °C for 1 day. The surface grafting structures of the zwitterionic PVDF membranes were characterized by X-ray photoelectron spectroscopy (XPS). XPS analysis was performed using a Thermal Scientific K-Alpha spectrometer equipped with a monochromated Al K X-ray source (1,486.6 eV photons). The energy of emitted electrons was measured with a hemispherical energy analyzer at pass energies ranging from 50 to 150 eV. All data were collected at a photoelectron takeoff angle of 45° with respect to the sample surface. The binding energy (BE) scale is referenced by setting the peak maximum in the C 1s spectrum to 284.6 eV. The high-resolution C 1s spectrum was fitted using a Shirley background subtraction and a series of Gaussian peaks. Water contact angles were measured with an Goniometer (Automatic Contact Angle Meter, Model FTA1000, First Ten Ångstroms Co, Ltd. USA) at 25 °C. The DI water was dropped on the sample surface at 10 different sites. The surface morphology of virgin and these zwitterionic PVDF membranes were examined by bioatomic force microscopy (bio-AFM). All AFM images were acquired with a JPK Instruments AG multimode NanoWizard (Germany). The instrument is equipped with a NanoWizard scanner and operated in air and liquid. For tapping-mode AFM, a commercial Si cantilever (TESP tip) of about 320 kHz resonant frequency from JPK was used. The relative humidity was less than 40%.

Protein Adsorption on the Zwitterionic PVDF Membranes. In this study, the adsorption of human fibrinogen on the membranes was evaluated using the enzyme-linked immunosorbent assay (ELISA) according to the standard protocol described briefly below. First, the membranes with a surface area of 0.4 cm^2 were placed in individual wells of a 24-well tissue culture plate, and each well was equilibrated with 1000 μL of PBS for 60 min at 37 °C. Then, the membranes were soaked in 500 μL of fibrinogen solution with a concentration of 1 mg/mL. After 180 min of incubation at 37 °C, the membranes were rinsed five times with 500 μL of PBS and then incubated in bovine serum albumin (BSA, purchased from Aldrich) for 90 min at 37 °C to block the areas unoccupied by protein. The membranes were rinsed with PBS five more times, transferred to a new plate, and incubated in a 500 μL PBS solution. The membranes were incubated with a primary monoclonal antibody that reacted with the fibrinogen for 90 min at 37 °C and then were blocked with 10 mg/mL BSA in PBS solution for 24 h at 37 °C. The membranes were subsequently incubated with the secondary monoclonal antibody, horseradish peroxidase (HRP)-conjugated immunoglobulins, for 60 min at 37 °C. The membranes were rinsed five times with 500 μL of PBS and transferred into clean wells, followed by the addition of 500 μL of PBS containing 1 mg/mL chromogen of 3,3′,5,5′-tetramethylbenzidine, 0.05 wt % Tween 20, and 0.03 wt % hydrogen peroxide. After incubation for 20 min at 37 °C, the enzyme-induced color reaction was stopped by adding 500 μL of 1 mmol/mL H_2SO_4 to the solution in each well, and finally, the absorbance of light at 450 nm was determined by a microplate reader. Protein adsorption on the membranes was normalized with respect to that on the virgin PVDF membrane as a reference. These measurements were carried out six times for each membrane ($n = 6$).

Blood Platelet Adhesion on the Zwitterionic PVDF Membranes. The PVDF membranes with a surface area of 0.4 cm^2 were placed in individual wells of a 24-well tissue culture plate, and each well was equilibrated with 1000 μL of phosphate buffered solution (PBS) for 2 h at 25 °C. Blood was obtained from a healthy human volunteer. Platelet rich plasma (PRP) containing approximately 1×10^5 cells/mL was prepared by centrifugation of the blood at 1200 rpm for 10 min. The platelet concentration was determined by microscopy (NIKON TS 100F). To test the activated platelet adhesion on the membranes, 200 μL of the PRP, first recalcified by the addition of calcium (1 M $CaCl_2$, 5 μL), was placed on the PVDF surface in each well of the tissue culture plate and incubated for 120 min at 37 °C. After the membranes were rinsed twice with 1000 μL of PBS, they were immersed into 2.5% glutaraldehyde of PBS for 48 h at 4 °C to fix the adhered platelets and adsorbed proteins. Then, they were rinsed two times with 1000 μL of PBS and gradient-dried with ethanol in 0% v/v PBS, 10% v/v PBS, 25% v/v PBS, 50% v/v PBS, 75% v/v PBS, 90% v/v PBS, and 100% v/v PBS for 20 min at each step and dried in air. Finally, the samples were sputter-coated with gold prior to observation with a JEOL JSM-5410 SEM operating at 7 keV.

Plasma-Clotting Time of the Zwitterionic PVDF Membranes. The anticoagulant activities of the prepared membranes were evaluated by testing plasma-clotting time in human plasma. Prior to the test, the membranes with one side area of 0.4 cm^2 (0.36 cm in radius and a total contact area of 0.8 cm^2) were placed into the 24-well plate. Human normal plasma (platelet poor) was prepared from anticoagulated human blood from three donors by centrifugation (1200 rpm for 10 min at 25 °C followed by 3000 rpm for 10 min at 25 °C). Plasma was recalcified to 20 mM $CaCl_2$ by the addition of calcium from a 1 M stock solution and shaken for 30 s at 37 °C. Then, 0.5 mL plasma was immediately added to each well in a 24-well plate (Falcon, nontissue culture treated polystyrene). The clotting time of the plasma was determined as the time where the onset of the absorbance transition, which was indicated by reading the absorbance at 660 nm using the PowerWave microplate spectrophotometer with a programmed temperature control of 37 °C. Each clotting time is reported as the average value of repeated measurements of six samples ($n = 6$).

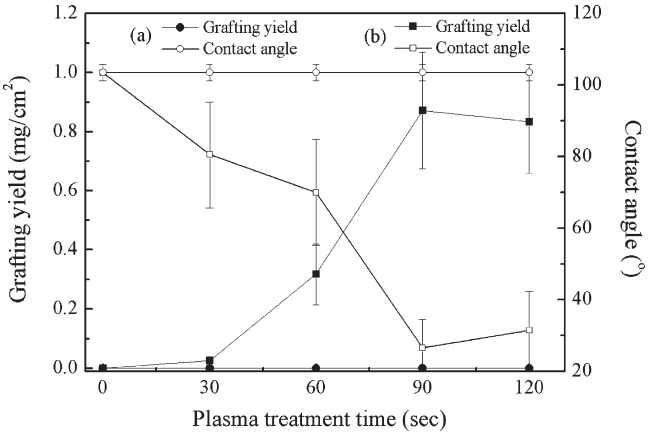

Figure 2. Changes in the surface grafting yield and water contact angle of PVDF-*g*-PSBMA membranes as a function of plasma treatment time (a) without and (b) with pretreatment of argon low-pressure plasma.

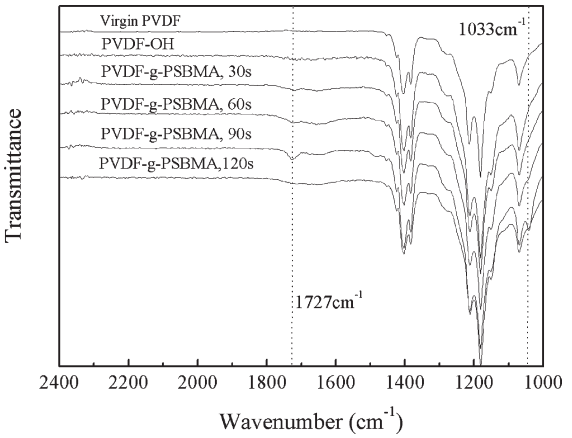

Figure 3. FT-IR spectra of the virgin PVDF membrane and PVDF membranes with a grafted PSBMA layer and plasma treatment times of 30, 60, 90, and 120 s.

Red Blood Cell Hemolysis of the Zwitterionic PVDF Membranes. The membrane disruption of red blood cells (RBCs) was estimated to determine the nonfouling characteristics of the prepared membranes using a RBC hemolysis assay. The protocol used to isolate and purify the red blood cells and to quantify hemolysis has been described in previous work.[22] RBCs were isolated by blood centrifugation and washed three times with a 0.15 M saline solution. In each hemolysis experiment, 10^8 RBCs were suspended in 500 μL of PBS. Prior to the test, the membranes with a surface area of 0.4 cm^2 were placed into the 24-well plate, and 500 μL of RBC solution was added. The membrane and RBC mixtures were incubated in a 37 °C water bath for 60 min. The mixed solution was then centrifuged for 5 min at 2000 rpm to separate intact RBCs and disrupted membranes from the solution. The absorbance of the supernatant containing the released hemoglobin (Hb) was then measured at 541 nm using the PowerWave microplate spectrophotometer. One hundred percent hemolysis was determined by measuring the absorbance of 10^8 RBCs with complete lysis by suspending them in DI water. The control was 10^8 RBCs in PBS. Each hemolysis is reported as the average value of repeated measurements of six samples (n = 6).

RESULTS AND DISCUSSION

Surface Copolymerization and Characterization. In general, the surface coverage of the PSBMA-grafted layer on PVDF (PVDF-*g*-PSBMA) membranes can initially be regulated by the amount of uniform-coated SBMA monomer and the plasma treatment time. The PVDF membrane coated with SBMA monomer of ~2.0 mg/cm^2 was directly treated by atmospheric plasma by varying the plasma treatment time from 30 to 120 s. However, the coating uniformity of SBMA monomer on the hydrophobic PVDF surface was found to result in dramatically poor spatial distribution and to form the droplet shrinkage of SBMA that may be due to the large difference in surface polarity between SBMA and PVDF. In Figure 2a, results showed that there is no variation in the surface grafting yield and water contact angle of PVDF-*g*-PSBMA membranes at any time during plasma treatment, indicating no PSBMA polymers were immobilized on the PVDF membrane surface. The mechanism of plasma-induced surface copolymerization can be divided into two reaction stages. In the initial stage, energetic species (Ar metastables and ions) and UV radiation from the plasma treatment generate initiator radicals both in the SBMA monomer and on the PVDF membrane surface. Then, the initiator radicals may undergo two types of additional reactions, including copolymerization of the initiator radicals on the PVDF membrane surface to the SBMA monomers or the polymerization of initiator radicals in the SBMA monomer to the SBMA monomer. The first type is a critical reaction that results in the immobilization of PSBMA polymers from the PVDF membrane surface. As illustrated in Figure 1, an integrated process of plasma-induced surface copolymerization of zwitterionic PSBMA was developed to modify the hydrophobic PVDF membrane with a highly polar PSBMA-grafted layer. First, the virgin PVDF membrane was pretreated by low-pressure plasma with argon and followed by the incubation of DI water at 60 °C to generate the hydroxyl groups, resulting in a decrease in the water contact angle from 120 to 105° and an increase in the chemical compatibility between SBMA and PVDF. Then, the following step is plasma-induced surface copolymerization of the PVDF membrane with a uniform-coated SBMA monomer layer of ~2.0 mg/cm^2 via atmospheric plasma treatment. In Figure 2b, results showed that the grafting yield of the PSBMA graft layer on the surface of PVDF membranes increased as the plasma treatment time increased from 30 to 120 s. The reduced water contact angles indicate that the surface hydrophilicity of PVDF-*g*-PSBMA membranes increases with increasing surface coverage of grafted PSBMA polymer on the hydrophobic PVDF membranes. The water contact angle of the PVDF-*g*-PSBMA membrane surface was as low as approximately 30°, which indicates an obvious increase in hydrophilicity compared to the virgin PVDF membrane surface. Moreover, the water contact angle remained almost unchanged for grafting yields above 0.8 mg/cm^2, which indicates that grafted PSBMA polymer on the PVDF membrane surface approaches its respective saturated coverage with a steady water contact angle.

The presence of grafted PSBMA polymer on the PVDF membrane surface is characterized by an FT-IR measurement; a typical spectrum is shown in Figure 3. The presence of the grafted polySBMA could be ascertained from the ester carbonyl groups and the sulfonate groups observed from the bands of the O−C═O stretch at 1727 cm^{-1} and $-SO_3$ stretch at 1033 cm^{-1}, respectively, which appear on the PSBMA-grafted PVDF membranes. It was found that both the intensity of the O−C═O and $-SO_3$ adsorption increased as the starting plasma treating time

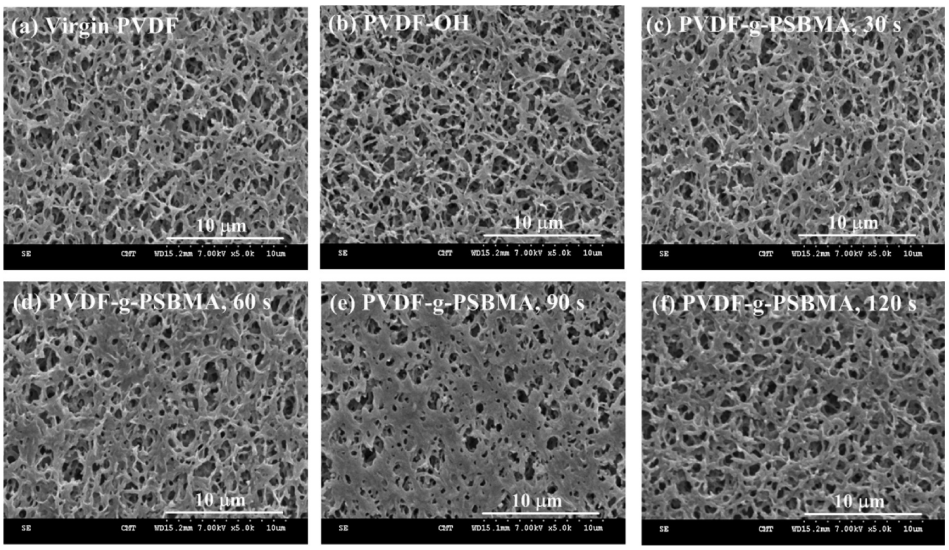

Figure 4. SEM images of the surface morphology of the modified PVDF membranes with grafted PSBMA: (a) virgin PVDF membrane; (b) PVDF−OH membrane; (c−f) the PVDF-*g*-PSBMA membranes with plasma treatment times of 30, 60, 90, and 120 s, respectively. All images are magnified 1000×.

was increased from 30 to 90 s. The result indicates that the growth of the grafted PSBMA polymer depends on the grafting time during atmospheric plasma treatment. However, after the surface plasma treatment at 120 s, it was found that the decreased intensity of the O−C═O and $-SO_3$ adsorption indicates significant degradation of the grafted PSBMA layer on the PVDF membrane.

Surface Morphology of the Zwitterionic PVDF Membranes. The surface morphology of the PVDF-*g*-PSBMA membranes is associated with the surface coverage of grafted PSBMA polymer on the PVDF membrane, which was observed by SEM and AFM. In Figure 4, the surface coverage of the PVDF-*g*-PSBMA membrane revealed an obvious change as the plasma treatment time was increased from 30 to 120 s. After the surface plasma treatment at 90 s, the SEM surface images in Figure 4e reveal that the porous structure on the PVDF membrane surface was almost covered with the grafted PSBMA layer. The grafted amount of PSBMA obtained from the measurements of the [O−C═O]/[C−F] ratio characterized by FT-IR increased as the plasma treatment time increased from 30 to 90 s, which was consistent with the changes in morphology on the PVDF-*g*-PSBMA membrane surface that were evident in SEM images. The results clearly indicate that the decrease in the water contact angle on the membrane surface was due to the increase in surface coverage of the grafted PSBMA layer. After the surface plasma treatment for 120 s, Figure 4f shows that the degradation effects on the grafted PSBMA layer resulted in the etching structures of the PVDF-*g*-PSBMA membrane, which was also ascertained by an FT-IR measurement.

The surface roughness of grafted PSBMA polymer on the PVDF membrane surfaces was observed by AFM. In Figure 5, the surface morphology and roughness of the PVDF-*g*-PSBMA membrane surface revealed an obvious change associated with the plasma treatment time of surface copolymerization. From the short plasma treatment at 30 s, the grafted PSBMA polymer on the PVDF membrane showed an obvious increase of approximately 235 nm in the surface rms roughness, which may be due to the incomplete plasma-induced surface copolymerization. As the surface plasma treatment was extended from 60 to 120 s, the surface rms roughness had a dramatic decrease of approximately 85 nm, which indicates the formation of the uniform grafted PSBMA surface for the prepared membrane of PVDF-*g*-PSBMA. The results indicate that the surface roughness of grafted PSBMA polymer on PVDF membrane surface is associated with plasma treatment time when atmospheric plasma-induced treatment is used. The AFM results suggest that atmospheric plasma-induced surface copolymerization is a well-controlled process to prepare a zwitterionic PVDF membrane surface with a uniform distribution of a highly polar PSBMA layer.

Correlation of Surface Hydrophilicity and Grafting Structure of the Zwitterionic PVDF membranes with Protein Adsorption. In general, it was believed that the ability of a membrane surface to resist plasma protein adsorption, such as fibrinogen, is a prerequisite for a membrane surface to resist blood platelet adhesion.[12,13] Therefore, the adsorption of fibrinogen to a membrane usually provides a good indication of the membrane performance of the hemocompatibility. The formation of the bounded water layer on a highly hydrated surface was considered to be crucial to repel plasma proteins and generate the antithrombogenic surface.[33,34] In general, the increase in surface grafting coverage associated with the increase in the thickness of the PSBMA layer resulted in the almost constant water contact angle, which indicates the grafted PSBMA polymer on the PVDF membrane surface approaches its respective saturated coverage with a steady water contact angle. However, it should be noted that the change in water contact angle is usually not a good indication of the degree of hydration on the highly hydrophilic surface coverage. The surface thickness of the grafted PSBMA polymer is associated with the capacity of water molecules on the hydrated surface. In this study, the hydration capacity (mg/cm^2) of the prepared membrane is defined as the difference in wet weight between the PSBMA grafted PVDF membrane and the virgin PVDF membrane divided by the total surface area of the virgin PVDF membrane. Figure 6 shows that the dependence of the relative fibrinogen adsorption and hydration capacity of the modified PVDF membranes on the surface grafting yield of

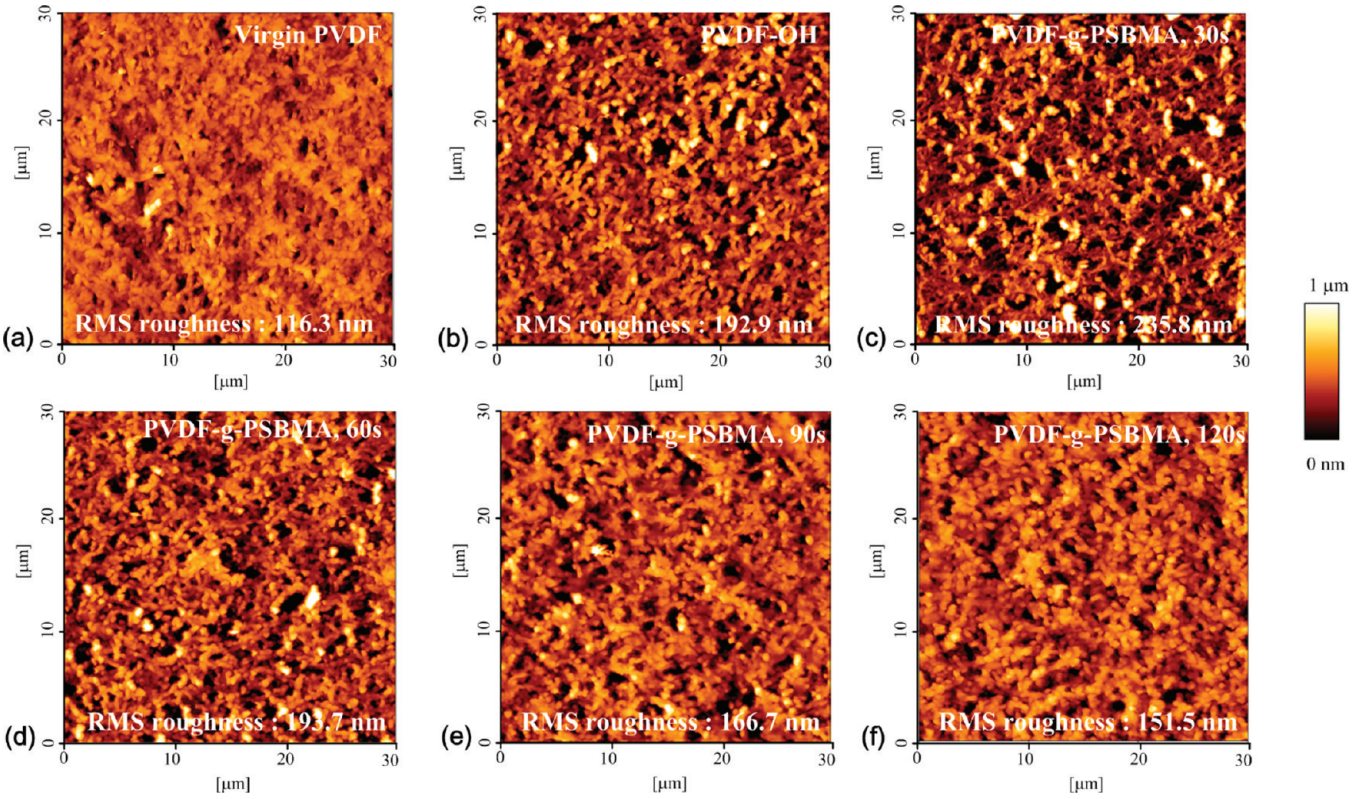

Figure 5. Tapping-mode AFM of surface rms roughness of the modified PVDF membranes with grafted PSBMA: (a) virgin PVDF membrane; (b) PVDF−OH membrane; (c−f) the PVDF-*g*-PSBMA membranes with plasma treatment times of 30, 60, 90, and 120 s, respectively. The dimensions of the scan images are 30.0 μm × 30.0 μm with a Z scale of 1 μm.

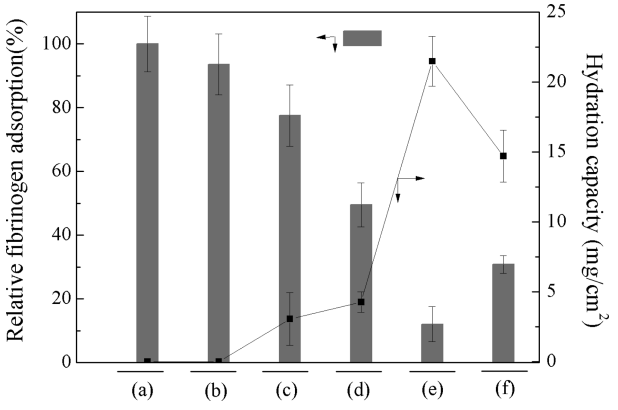

Figure 6. Changes in the relative fibrinogen adsorption and hydration capacity of the modified PVDF membranes with PSBMA: (a) virgin PVDF membrane; (b) PVDF−OH membrane; (c−f) the PVDF-*g*-PSBMA membranes with plasma treatment times of 30, 60, 90, and 120 s, respectively.

PSBMA layer can be controlled by the plasma treatment time. The increase in grafting yield associated with the increase in the thickness of the PSBMA layer resulted in the reduced adsorption of human fibrinogen and the increased hydration capacity. It was found that reduction in nonspecific fibrinogen adsorption exhibited a positive correlation with the variation of the hydration capacity of PVDF-*g*-PSBMA membranes. Protein resistance and hydration capacity were maximized when the plasma treatment time of grafted PSBMA was 90 s; the relative protein adsorption on PVDF-*g*-PSBMA is effectively reduced to ~10% of that on virgin PVDF as the hydration capacity increases to 22 mg/cm^2. However, a plasma treatment time of 120 s with a similar grafting yield and contact angle to the case at 90 s generated relative less protein resistance by ~35%, and the hydration capacity was reduced to 15 mg/cm^2. The results may be associated with the chemical degradation of the grafted PSBMA layer on the PVDF membrane, which is revealed by the FT-IR and SEM measurements.

Our previous study showed that it is important to maintain the electrical neutrality of the grafted zwitterionic polymer by minimizing the electrostatic interactions with plasma proteins.[21] The inflection point in the dependence of nonspecific fibrinogen adsorption and hydration capacity on plasma treatment time may result from the overall balance of charged moieties distributed in the grafted PSBMA layer in the PVDF membrane surface. The charge ratio of positively and negatively charged moieties in the PSBMA layer was determined by the ratio of the atomic percentages of nitrogen and sulfur (N/S), as shown in Figure 7. From the surface compositional analysis of the PVDF membrane coated with SBMA monomer in Figure 7b, the peaks of nitrogen and sulfur are found to be at almost equal quantities; the calculated N/S ratio of 0.98 indicates that the zwitterionic SBMA monomer is electrically neutral. Thus, the N/S ratio is a good indicator to determine the plasma treatment time that causes the formation of a homogeneous charge-balanced distribution in the grafted PSBMA layer on PVDF membrane surface. It can be seen that the N/S ratio approached 1.0 as the plasma treatment time was increased from 30 to 90 s, resulting in the formation of an overall balance of charged moieties in the grafted PSBMA layer based on the calculated N/S ratio of 1.02. However, the N/S ratio

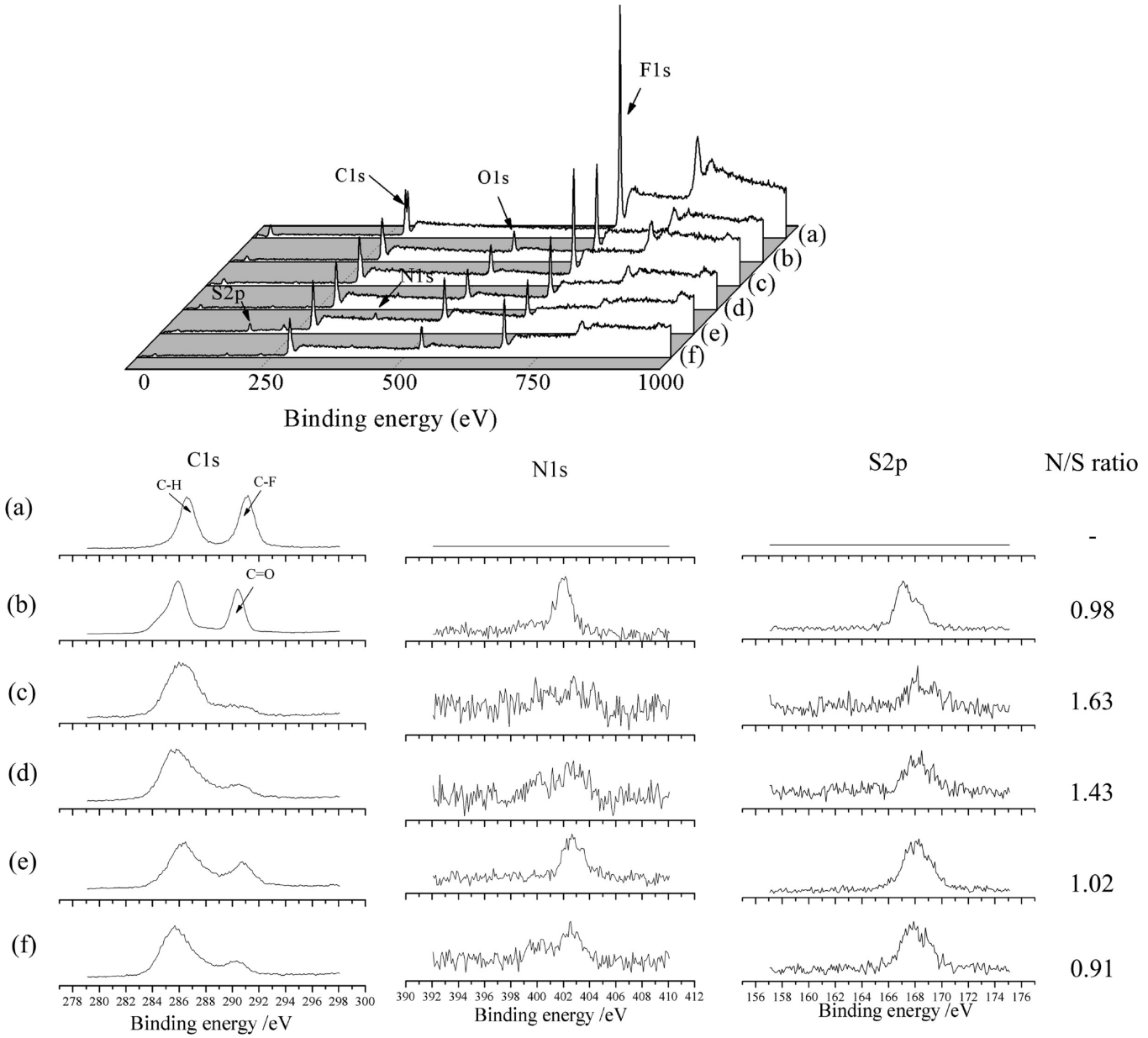

Figure 7. XPS spectra of the modified PVDF membranes with PSBMA in C1s, N1s, and S2p regions: (a) virgin PVDF membrane; (b) PVDF membrane coated with SBMA monomer; (c−f) the PVDF-*g*-PSBMA membranes with plasma treatment times of 30, 60, 90, and 120 s, respectively.

decreased to 0.91 as the plasma treatment time was further increased to 120 s, resulting in low protein resistance and reduced hydration capacity. It was found that even a slight charge bias in the grafted zwitterionic PSBMA layer can induce electrostatic interactions between proteins and the membrane surfaces, leading to surface protein adsorption. The results also indicate that the reduction of protein adsorption on the PVDF-*g*-PSBMA surfaces was associated with the charge ratio, which depended on the amounts of nitrogen and sulfur in the grafted PSBMA layer, which in turn depended on the plasma-induced copolymerization conditions. These results suggest that the general evaluation of protein adsorption on the PVDF-*g*-PSBMA membrane surfaces should consider not only the surface hydrophilicity and hydration capacity but also the charge balance of the grafted PSBMA polymer layer.

Surface Hemocompatibility of the Zwitterionic PVDF membranes. Previous works showed that the adhesion and activation of platelets from the bloodstream may be correlated with the adsorption of fibrinogen on surfaces.[18,21] As the membrane surfaces come into contact with blood, even 10 ng/cm^2 of adsorbed fibrinogen may induce a full scale blood platelet adhesion, leading to thrombosis and embolism at the blood-contacting side of membrane surfaces in the bloodstream.[12,13] Figure 8 shows SEM images, at a magnification of 1000×, of the prepared membranes in contact with recalcified PPP solution for 120 min at 37 °C in vitro. The SEM results showed the formation of thrombosis on the virgin PVDF and PVDF−OH membranes with full-scale platelet adhesion and activation at the blood-contact site. However, there also slightly activated platelets on the PVDF-*g*-PSBMA membrane surfaces clearly appeared with positive-rich charges when the plasma treatment time was 30 and 60 s. It was shown that no platelets adhered to the PVDF-*g*-PSBMA membrane surface with overall electric neutrality, as

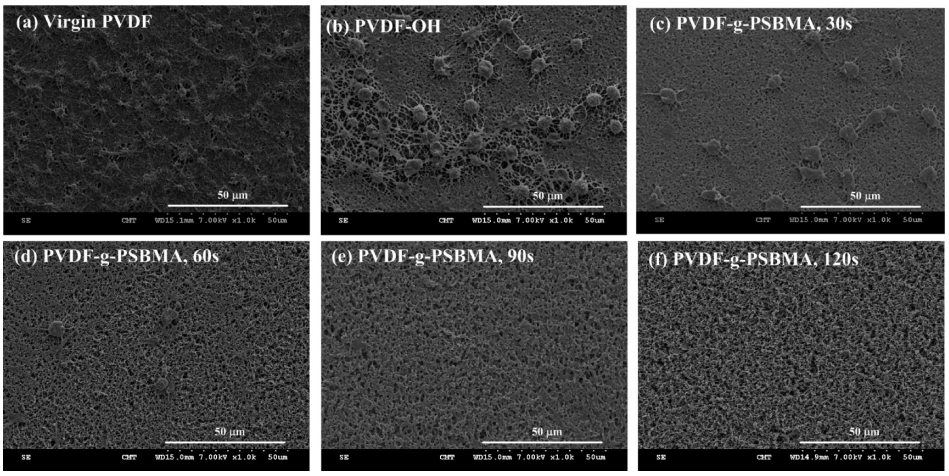

Figure 8. SEM images of platelets adhered onto the surface of the modified PVDF membranes with grafted PSBMA: (a) virgin PVDF membrane; (b) PVDF−OH membrane; (c−f) the PVDF-*g*-PSBMA membranes with plasma treatment times of 30, 60, 90, and 120 s, respectively. All images are magnified 1000×.

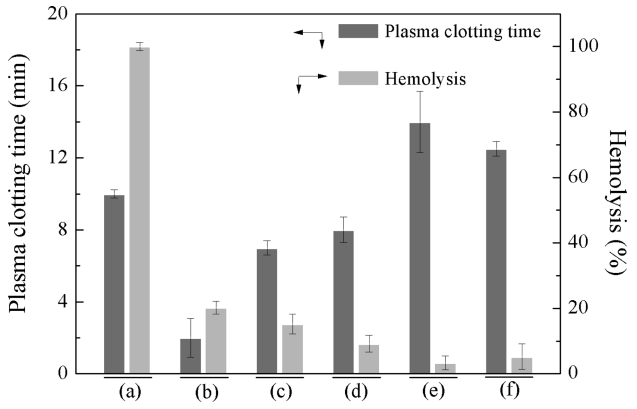

Figure 9. Plasma clotting time of recalcified platelet-poor plasma and hemolysis of RBC solution in the presence of modified PVDF membranes with grafted PSBMA: (a) blank PS wells; (b) virgin PVDF membrane; (c−f) the PVDF-*g*-PSBMA membranes with plasma treatment times of 30, 60, 90, and 120 s, respectively. Clotting time for blank PS wells was approximately 10 min at 37 °C. Each plasma clotting time and hemolysis test is an average of six samples.

shown in Figure 8e. The results confirmed the previous hypothesis that a nanometer-scale homogeneous, charge-balanced surface from zwitterionic groups can provide excellent blood compatibility at human body temperature.[21] It should be noted that no platelets adhered to the PVDF-*g*-PSBMA membrane surface with partially negative-rich charges as shown in Figure 8f, which may be due to the interfacial repulsion from the negatively charged nature of the cell membrane of platelets.

The measurement of plasma clotting has already become a recognized test to estimate the blood compatibility of a prepared membrane interface.[6] The prepared PVDF-*g*-PSBMA membranes were directly incubated with human plasma to determine the effects of direct-contact activation on polymer-induced plasma clotting as evaluated by their recalcified-plasma-clotting times. In this work, the percentage of the tested membrane area in contact with recalcified platelet-poor plasma is approximately 30%. Thus, 0.4 cm^2 of each prepared membranes was incubated with 0.5 mL of recalcified human PPP solution in a PS 24-well plate at body temperature of 37 °C. It is important to control the percentage of the PS well area in contact with the testing media. Maintaining balance of the area ratio of the tested membrane and the PS well is important to show the meaningful and obvious scale of plasma-clotting time. As shown in Figure 9a, plasma clotting for the recalcified plasma solutions in blank PS wells was determined to have an upper limit of plasma-clotting time of approximately 10 min at 37 °C for the protocol used. When the recalcified PPP solution was added to the virgin PVDF membrane, the clotting time decreased to ∼2.5 min, indicating that hydrophobic PVDF is an easily activated membrane that activates plasma clotting through its intrinsic coagulation pathway. The average clotting time increased with an increase in plasma treatment time, which is attributed the surface hydration of grafted PSBMA layers on the PVDF membrane surface. For the PVDF-*g*-PSBMA membrane surfaces with positive-rich charges, when the plasma treating time was 30 and 60 s, the plasma-clotting time was shortened to 7−8 min at 37 °C; it generated faster activation in plasma than the recalcified plasma solutions in blank PS wells. The decrease in clotting time for positively charged PVDF-*g*-PSBMA membranes may be associated with fibrinogen adsorption onto the membrane surfaces in a single-protein solution revealed by the ELISA measurement at 37 °C, as shown in Figure 6. It is interesting to observe that when the plasma treatment time was 120 s, the average clotting time increased to ∼12.5 min, indicating an anticoagulant property of the PVDF-*g*-PSBMA membrane with slightly negative-rich charges. As shown in Figure 9e, for the PVDF-*g*-PSBMA membrane surfaces with overall charge neutrality, the plasma-clotting time was further prolonged to ∼14 min at 37 °C. Plasma-clotting time and anticoagulant activity were maximized when the plasma treatment time was at 90 s, which clearly indicates that the PVDF-*g*-PSBMA membrane has a charge-balanced dependence on anticoagulant activity or contact activation to prevent or activate, respectively, plasma clotting in human blood. The inflection point in the dependence of anticoagulant activity on PVDF-*g*-PSBMA membranes may be due to the formation of the bounded water layer on a well-hydrated zwitterionic PSBMA layer with overall charge neutrality.

To further evaluate the bias influence of positive and negative charges on blood compatibility of prepared zwitterionic

PVDF-*g*-PSBMA membranes, a RBC hemolysis assay was performed. The observed hemolysis of RBCs in DI water at 37 °C was used as a control and is shown in Figure 9a. The observed hemolytic activity of PVDF-*g*-PSBMA membranes at a given plasma treating time was normalized to that of the reference control, DI water. The hemolytic activity of a virgin PVDF membrane was also tested for comparison. In general, hydrophobic surfaces are capable of interacting with biological membranes, causing disruption. Thus, it was observed that the virgin PVDF membrane exhibited ~20% hemolytic activity. In general, no apparent hemolytic activity was observed for the reference heparin in PBS (less than 1%). It is interesting to observe that the hemolytic activity exhibits was minimal for the PVDF-*g*-PSBMA membrane surfaces with overall charge neutrality at a specific plasma treatment time of 90 s, which indicates the good nonfouling nature of the zwitterionic layers with antihemolytic activity that can resist the disruption of blood cell membranes (approximately 3%). However, the PVDF-*g*-PSBMA membranes with positive-rich charges in RBC solution at physiologic conditions showed relative strong hemolysis (approximately 9−15%), indicating that the positive-bias nature of a zwitterionic surface with hemolytic activity enhances the disruption of blood cell membranes. These results suggest that the well-hydrated surface of PSBMA-grafted PVDF membranes with charge neutrality prepared by atmospheric plasma-induced surface copolymerization can efficiently reduce protein adsorption, suppress platelet adhesion/activation, and increase its hemocompatibility.

CONCLUSION

In this work, blood compatible zwitternionic PVDF membranes with controllable grafting coverage and a charge balance of grafted PSBMA layers were obtained via atmospheric plasma-induced surface copolymerization. Surface grafting structures of zwitterionic PSBMA layers with positive-rich charges, negative-rich charges and neutral electric charges on PVDF membranes were achieved using different plasma treatment times. For the first time, this study has shown that a grafted zwitterionic PSBMA layer on the PVDF membrane surface using the integrated plasma technique is a promising approach for the preparation of a blood compatible membrane with well-controlled overall charge neutrality. The blood compatibility of the zwitterionic PVDF-*g*-PSBMA membranes in human blood was characterized by human fibrinogen adsorption and blood-platelet adhesion and by recalcified plasma-clotting time and red blood cell hemolysis at physiological temperature. The results showed that PVDF-*g*-PSBMA membranes exhibited a antifouling property for plasma-protein and blood-platelet resistance that strongly depended on the surface hydrophilicity and charge-bias of the zwitterionic PSBMA layer on the PVDF membranes. The membrane with surface-grafted electrically neutral PSBMA layer presented excellent anticoagulant activity in human blood, which was attributed to the formation of a strong interfacial hydration layer and minimal electrostatic interaction between membrane interfaces and blood components. This study suggests that the zwitterionic PVDF membranes generated by controlling the charge neutrality of grafted PSBMA structures from atmospheric plasma-induced surface copolymerization have great potential in the surface modification of general hydrophobic membranes for use in human blood.

AUTHOR INFORMATION

Corresponding Author

*E-mail: ychang@cycu.edu.tw. Phone: 886-3-265-4122. Fax: 886-3-265-4199.

ACKNOWLEDGMENT

The authors wish to express their sincere gratitude to the Center-of-Excellence (COE) Program on Membrane Technology from the Ministry of Education (MOE), R.O.C., and the National Science Council (NSC 99-2321-B-033-003) for their financial support.

REFERENCES

(1) Harris, J. M. *Poly(Ethylene Glycol) Chemistry: Biotechnical and Biomedical Applications*, 1st ed.; Springer: New York, 1992.
(2) Holmlin, R. E.; Chen, X. X.; Chapman, R. G.; Takayama, S.; Whitesides, G. M. *Langmuir* **2001**, *17*, 2841–2850.
(3) Ratner, B. D.; Hoffman, A. D.; Schoen, F. D.; Lemons, J. E. *Biomaterials Science, an Introduction to Materials in Medicine*, 2nd ed.; Elsevier: Amsterdam, 2004.
(4) Iwasaki, Y; Ishihara, K. *Anal. Bioanal. Chem.* **2005**, *381*, 534–546.
(5) Chang, Y.; Chen, S. F.; Zhang, Z.; Jiang, S. Y. *Langmuir* **2006**, *22*, 2222–2226.
(6) Zhang, Z.; Zhang, M.; Chen, S. F.; Horbett, T. A.; Ratner, B. D.; Jiang, S. Y. *Biomaterials* **2008**, *29*, 4285–4291.
(7) Chen, S.; Jiang, S. Y. *Adv. Mater.* **2008**, *20*, 335–338.
(8) Xu, F. J.; Neoh, K. G.; Kang, E. T. *Prog. Polym. Sci.* **2009**, *34*, 719–761.
(9) Jiang, S. Y.; Cao, Z. Q. *Adv. Mater.* **2010**, *22*, 920–932.
(10) Rana, D.; Matsuura, T. *Chem. Rev.* **2010**, *110*, 2448–2471.
(11) Ratner, B. D. *Biomaterials* **2007**, *28*, 5144–5147.
(12) Shen, M. C.; Wagner, M. S.; Castner, D. G.; Ratner, B. D.; Horbett, T. A. *Langmuir* **2003**, *19*, 1692–1699.
(13) Kwak, D.; Wu, Y. G.; Horbett, T. A. *J. Biomed. Mater. Res., Part A* **2005**, *74A*, 69–83.
(14) Ishihara, K.; Ueda, T.; Nakabayashi, N. *Polym. J.* **1990**, *22*, 355–360.
(15) Zhang, Z.; Chen, S. F.; Chang, Y.; Jiang, S. Y. *J. Phys. Chem. B* **2006**, *110*, 10799–10804.
(16) Zhang, Z.; Chao, T.; Chen, S. F.; Jiang, S. Y. *Langmuir* **2006**, *22*, 10072–10077.
(17) Chang, Y.; Chen, S.; Yu, Q.; Zhang, Z.; Bernards, M.; Jiang, S. *Biomacromolecules* **2007**, *8*, 122–127.
(18) Chang, Y.; Liao, S. C.; Higuchi, A.; Ruaan, R. C.; Chu, C. W.; Chen, W. Y. *Langmuir* **2008**, *24*, 5453–5458.
(19) Chiang, Y. C.; Chang, Y.; Higuchi, A.; Chen, W. Y.; Ruaan, R. C. *J. Membr. Sci.* **2009**, *339*, 151–159.
(20) Chang, Y.; Chen, W. Y.; Yandi, W.; Shih, Y. J.; Chu, W. L.; Liu, Y. L.; Chu, C. W.; Ruaan, R. C.; Higuchi, A. *Biomacromolecules* **2009**, *10*, 2092–2100.
(21) Chang, Y.; Shu, S. H.; Shih, Y. J.; Chu, C. W.; Ruaan, R. C.; Chen, W. Y. *Langmuir* **2010**, *26*, 3522–3530.
(22) Shu, S. H.; Chang, Y. *Langmuir* **2010**, *26*, 17286–17294.
(23) Chang, Y.; Yandi, W.; Chen, W. Y.; Shih, Y. J.; Yang, C. C.; Ling, Q. D.; Higuchi, A. *Biomacromolecules* **2010**, *11*, 1101–1110.
(24) Yuan, J.; Lin, S.; Shen, J. *Colloids Surf., B* **2008**, *66*, 90–95.
(25) Liu, P. S.; Chen, Q.; Liu, X.; Yuan, B.; Wu, S. S.; Shen, J.; Lin, S. C. *Biomacromolecules* **2009**, *10*, 2809–2816.
(26) Liu, P. S.; Chen, Q.; Wu, S. S.; Shen, J.; Lin, S. C. *J. Membr. Sci.* **2010**, *350*, 387–394.
(27) Yang, Y. F.; Li, Y.; Li, Q. L.; Wan, L. S.; Xu, Z. K. *J. Membr. Sci.* **2010**, *362*, 255–264.
(28) Yang, C.; Sun, K.; Liu, J.; Wang, H.; Cao, Y. *Polym. Int.* **2010**, *59*, 1296–1302.
(29) Kang, E. T.; Zhang, Y. *Adv. Mater.* **2000**, *12*, 1481–1494.
(30) Wang, P.; Tan, K. L.; Kang, E. T.; Neoh, K. G. *J. Mater. Chem.* **2001**, *11*, 783–789.
(31) Guangqun, Z.; Toh, S. C.; Tan, W. L.; Kang, E. T.; Neoh, K. G. *Langmuir* **2003**, *19*, 7030–7037.
(32) Chang, Y.; Ko, C. Y.; Shih, Y. J.; Quémener, D.; Deratani, A.; Wang, D. M.; Lai, J. Y. *J. Membr. Sci.* **2009**, *345*, 160–169.

(33) He, Y.; Chang, Y.; Hower, J. C.; Zheng, J.; Chen, S. F.; Jiang, S. Y. *Phys. Chem. Chem. Phys.* **2008**, *36*, 5539–5544.
(34) He, Y.; Hower, J. C.; Chen, S. F.; Bernards, M. T.; Chang, Y.; Jiang, S. Y. *Langmuir* **2008**, *24*, 10358–10364.
(35) Wang, P.; Tan, K. L.; Kang, E. T.; Neoh, K. G. *J. Membr. Sci.* **2002**, *195*, 103–114.